ISSN 0020-1685, Inorganic Materials, 2018, Vol. 54, No. 10, pp. 1021–1026. © Pleiades Publishing, Ltd., 2018.
Original Russian Text © V.I. Pet'kov, A.S. Shipilov, E.Yu. Borovikova, A.M. Kovalskii, I.A. Stenina, A.B. Yaroslavtsev, 2018, published in Neorganicheskie Materialy, 2018, Vol. 54, No. 10, pp. 1079–1084.

# Synthesis, Structure, IR-Spectroscopic Characterization, and Ionic Conductivity of $Mg_{0.5}Zr_2(AsO_4)_x(PO_4)_{3-x}$

**V. I. Pet'kov**[a, *], **A. S. Shipilov**[a], **E. Yu. Borovikova**[b], **A. M. Kovalskii**[c], **I. A. Stenina**[d], **and A. B. Yaroslavtsev**[d]

[a]*Lobachevsky State University, pr. Gagarina 23, Nizhny Novgorod, 603950 Russia*
[b]*Moscow State University, Moscow, 119991 Russia*
[c]*Moscow Institute of Steel and Alloys (National University of Science and Technology), Leninskii pr. 4, Moscow, 119991 Russia*
[d]*Kurnakov Institute of General and Inorganic Chemistry, Russian Academy of Sciences, Leninskii pr. 31, Moscow, 119991 Russia*
**e-mail: petkov@inbox.ru*

Received March 12, 2018

**Abstract**—$Mg_{0.5}Zr_2(AsO_4)_x(PO_4)_{3-x}$ arsenate phosphates have been prepared by a sol–gel process and characterized by X-ray diffraction, IR spectroscopy, and impedance spectroscopy. The results indicate the formation of a continuous series of solid solutions with the $Sc_2(WO_4)_3$ structure (sp. gr. $P2_1/n$) in the composition range $0 < x < 3$. The unit-cell parameters of the solid solutions increase linearly with composition, as a consequence of arsenic substitution for phosphorus, which has a smaller ionic radius. The number of observed stretching and bending bands of the $AsO_4^{3-}$ and $PO_4^{3-}$ ions in the IR spectra of the solid solutions agrees with that predicted by factor group analysis for space group $P2_1/n$. The observed gradual shift of the absorption bands of the $AsO_4$ tetrahedra to lower frequencies with increasing arsenic content on the tetrahedral site supports the X-ray diffraction evidence of the formation of substitutional solid solutions. The cation conductivity of $Mg_{0.5}Zr_2(AsO_4)_x(PO_4)_{3-x}$ with $0 \le x \le 1$ has been shown to exceed the conductivity of the parent magnesium zirconium arsenate.

*Keywords:* magnesium zirconium arsenate phosphates, scandium tungstate structure, synthesis, X-ray diffraction, IR spectroscopy, impedance spectroscopy

**DOI:** 10.1134/S0020168518100138

## INTRODUCTION

Materials with the $Sc_2(WO_4)_3$ (SW) structure, analogs of NASICON solid ionic conductors, are known owing to the possibility of ion substitutions on all of their crystallographic sites, without changes in their structural basis [1, 2]. Targeted changes in the cation and anion compositions of such systems ensure the formation of chemically complex materials with tailored electrical, magnetic, thermophysical, optical, catalytic, and other properties [3].

One of the key properties of the materials with the SW structure is their ionic conductivity. It can be controlled owing to the flexibility of their structural framework and changes in the dimensions of conductive channels, which are determined by iso- and heterovalent substitutions for the framework-forming ions. Heterovalent substitutions that allow the SW structure to persist alter the occupancy of mobile ions on vacant sites in the crystal lattice. Partial substitutions of ions in lower oxidation states for structure-forming cations lead to an increase in the concentration of mobile ions on extra-framework sites and a rise in ionic conductivity [4–6]. Substitutions of ions in higher charge states lead to a targeted formation of an increased cation vacancy concentration [7]. High cation mobility in compounds with the SW structure, in combination with their chemical and thermal stability, suggests that they are promising materials.

Solid electrolytes based on ionic compounds with magnesium cation conductivity have attracted researchers' attention in the context of a possible transition from lithium ion batteries to magnesium ion batteries, which hold more promise because of their higher capacity due to the larger charge of the $Mg^{2+}$ ion (with a small difference in molecular mass between their compounds), the higher abundance of magnesium in the Earth's crust, and its low cost [8–10].

The $Mg_{0.5}Zr_2(PO_4)_3$ phosphate and $Mg_{0.9+0.5y}Zn_{0.4}Al_yZr_{1.6-y}(PO_4)_3$ ($y = 0.4$) and $Mg_{0.5+y}(Zr_{1-y}Fe_y)_2(PO_4)_3$ ($y = 0.4$) phases of variable composition have the SW structure, monoclinic unit cells, and 773 K magnesium ion conductivity from $10^{-5}$ to $10^{-4}$ S/cm [11–13]. Heterovalent substitutions of smaller cations in lower oxidation states (iron and aluminum) for zir-

**Table 1.** Best-fit polynomials of the form $p = p_2x^2 + p_1x + p_0$ for the unit-cell parameters ($a$, $b$, $c$, $\beta$, and $V$) of the $Mg_{0.5}Zr_2(AsO_4)_x(PO_4)_{3-x}$ ($0 < x < 3$) solid solutions

| Crystallographic parameter | $p_2$ | $p_1$ | $p_0$ |
|---|---|---|---|
| $a$ (±0.001 Å) | 0.0114 | 0.0753 | 12.488 |
| $b$ (±0.001 Å) | 0.007 | 0.0551 | 8.9478 |
| $c$ (±0.001 Å) | 0.0124 | 0.0547 | 8.8784 |
| $\beta$ (±0.01°) | 0.0129 | 0.0144 | 90.7491 |
| $V$ (±0.1 Å$^3$) | 3.4095 | 17.911 | 992.03 |

conium in the composition of these phosphates lead to an increase in the concentration of magnesium ions and a decrease in the size of conduction channels. Halim et al. [14] assumed the size of the structural channels in $Mg_{0.5}Zr_2(PO_4)_3$ to be too large for $Mg^{2+}$ migration and substituted $Si^{4+}$ ($r$ = 0.41 Å) for the framework-forming cation $Zr^{4+}$ ($r$ = 0.72 Å) in order to raise the ionic conductivity of the material. The highest electrical conductivity of the $Mg_{0.5}Si_2(PO_4)_3$ sample sintered at 1073 K was $1.83 \times 10^{-5}$ S/cm.

The effect of anion substitutions on the electrical conductivity of $Mg_{0.5}Zr_2(PO_4)_3$ have not been studied previously. At the same time, in a study of $LiZr_2(AsO_4)_x(PO_4)_{3-x}$ solid solutions with the SW structure, their lithium ion conductivity was observed to increase systematically when phosphorus was replaced by arsenic, having a larger ionic radius [15]. In view of this, it was of interest to examine the effect of the size of the conduction channels in $Mg_{0.5}Zr_2(PO_4)_3$ on its ionic conductivity.

In connection with this, the purpose of this work was to examine the effect of $P^{5+} \leftrightarrow As^{5+}$ isomorphous substitutions on the composition and temperature stability ranges, IR spectroscopic properties, and ionic conductivity of $Mg_{0.5}Zr_2(AsO_4)_x(PO_4)_{3-x}$ solid solutions.

## EXPERIMENTAL

$Mg_{0.5}Zr_2(AsO_4)_x(PO_4)_{3-x}$ samples with $x$ = 0, 1.0, 1.5, 2.0, and 3.0 were prepared by a sol–gel process followed by heat treatment. To this end, appropriate ratios of aqueous $MgCl_2$ and $ZrOCl_2$ solutions were poured together at room temperature with constant stirring. Next, solutions containing appropriate amounts of orthophosphoric and arsenic acids were added while stirring. The resultant gel was dried at 363 K and heat-treated in air at 873 and 1073 K for 24 h at each temperature, with several intermediate grindings.

The chemical composition and homogeneity of the samples were checked by X-ray microanalysis on a JEOL JSM-7600F field emission (Schottky cathode) scanning electron microscope (SEM). The microscope was equipped with an Oxford Instruments X-Max 80 (Premium) energy dispersive spectrometer system for X-ray microanalysis, with a semiconductor silicon drift detector. The elemental composition of the samples was determined with an accuracy of 2 mol %.

X-ray diffraction patterns of the samples were obtained on a Shimadzu XRD-6000 diffractometer (Cu$K_\alpha$ radiation, $\lambda$ = 1.54178 Å, angular range $2\theta$ = 10°–50°, scan step of 0.02°, continuous scan rate of 1°/min). X-ray diffraction data were used to determine the phase composition of the materials in the sample preparation process after each isothermal firing step and to ascertain whether the synthesized compounds were phase-pure. Unit-cell parameters were determined using indexed X-ray diffraction patterns.

IR spectra of the synthesized magnesium zirconium arsenate phosphates were measured at room temperature in the range 4000 to 400 cm$^{-1}$ on a Bruker IFS 125HR Fourier transform IR spectrometer equipped with a single-reflection diamond attenuated total reflection (ATR) module. The spectral resolution was 2 cm$^{-1}$.

Ionic conductivity was measured at frequencies from 10 Hz to 2 MHz and temperatures from 323 to 1033 K using an IPU-62 ac bridge. The samples had the form of pressed cylindrical pellets ($R$ = 5 mm, $h$ = 2 mm) with platinum contacts. The heating rate was 2 K/min. The conductivity was determined by extrapolating the semicircle representing the bulk component onto the real axis.

## RESULTS AND DISCUSSION

Single-phase polycrystalline $Mg_{0.5}Zr_2(AsO_4)_x(PO_4)_{3-x}$ samples, white in color, were obtained at 1073 K. X-ray diffraction data indicated the formation of a continuous series of solid solutions with the SW structure throughout the concentration range ($0 < x < 3$). The position of the diffraction peaks in the X-ray diffraction patterns of the solid solutions was found to vary gradually with composition (Fig. 1). The X-ray diffraction patterns were indexed using data for $Ni_{0.5}Zr_2(PO_4)_3$, a structural analog [16].

According to analysis of systematic absences in the X-ray diffraction patterns of the samples, the synthesized magnesium zirconium arsenate phosphates crystallize in space group $P2_1/n$. The unit-cell parameters of the continuous isomorphous $Mg_{0.5}Zr_2(AsO_4)_x(PO_4)_{3-x}$ solid solutions, determined after indexing their X-ray powder diffraction patterns, are given in Table 1.

According to the electron microscopy and electron probe X-ray microanalysis results, the samples were homogeneous and consisted of grains differing in shape. Analysis of micrographs of the samples led us to conclude that the grains ranged in size from 1 to 10 μm. Their compositions corresponded to the intended $x$ values to within the accuracy of the method. As an example, Fig. 2 shows a micrograph of the $x$ = 1.5 sample.

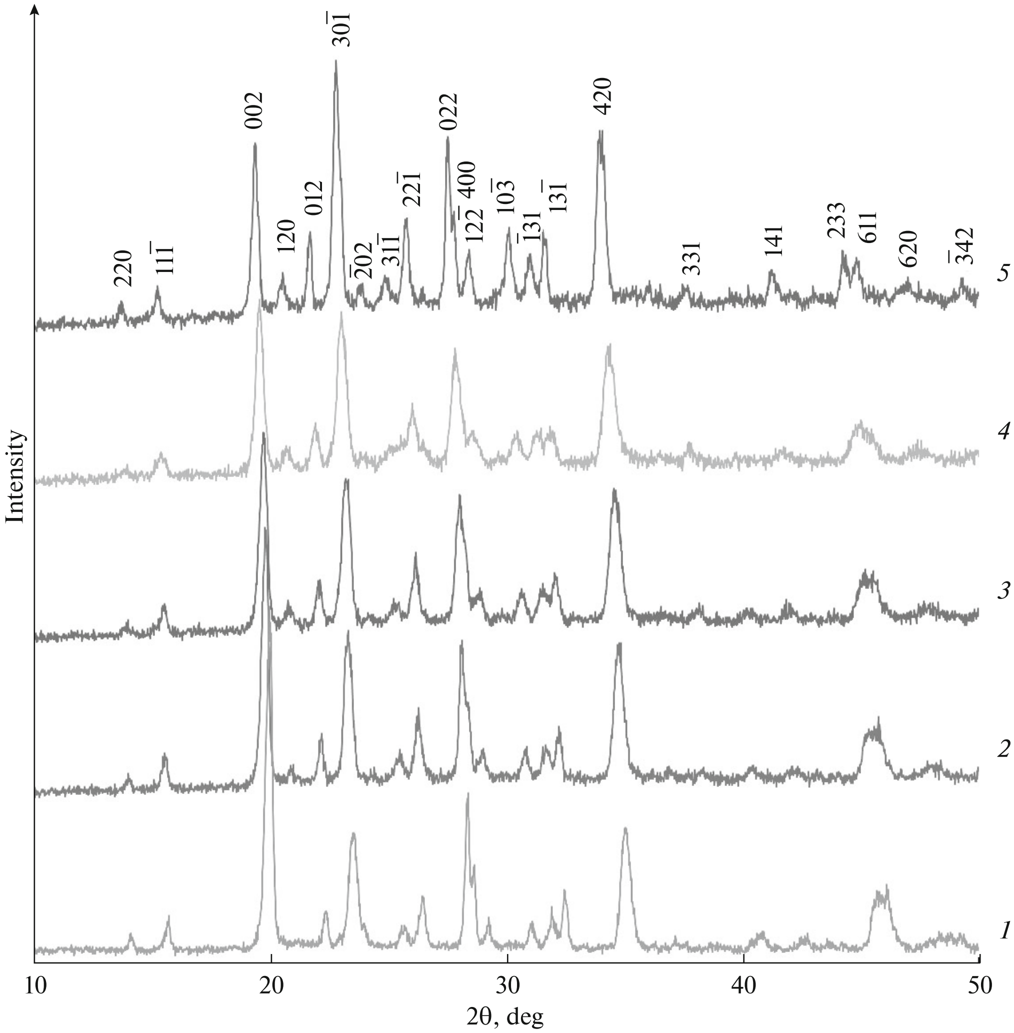

**Fig. 1.** X-ray diffraction patterns of the $Mg_{0.5}Zr_2(AsO_4)_x(PO_4)_{3-x}$ samples with $x$ = (*1*) 0, (*2*) 1.0, (*3*) 1.5, (*4*) 2.0, and (*5*) 3.0.

According to the electron probe X-ray microanalysis results, its chemical composition corresponded to the intended one, $Mg_{0.5}Zr_2As_{1.5}P_{1.5}O_{12}$, to within the accuracy of the method.

The $Mg_{0.5}Zr_2(AsO_4)_x(PO_4)_{3-x}$ samples with $x \geq 1$ were thermally unstable above 1073 K. The observed decomposition of the solid solutions was caused by the presence of larger sized arsenic ions on framework sites of the SW structure, which led to steric mismatch between the extra-framework sites and the magnesium ions occupying them.

Figure 3 shows IR spectra of the arsenate phosphates. The spectra of the $Mg_{0.5}Zr_2(PO_4)_3$ ($x = 0$) and $Mg_{0.5}Zr_2(AsO_4)_3$ ($x = 3$) end-members are characteristic of compounds with the SW structure and space group $P2_1/n$ [17, 18]. In their monoclinic structure, the phosphorus or arsenic atoms occupy three positions of $C1$ symmetry (4*e*). According to selection rules, their IR spectrum can contain eight stretching bands ($\nu_1$: $A_u + B_u$, $\nu_3$: $3A_u + 3B_u$) and ten bending bands ($\nu_2$: $2A_u + 2B_u$, $\nu_4$: $3A_u + 3B_u$) of the $PO_4^{3-}$ or $AsO_4^{3-}$ complex ion for each of the three independent

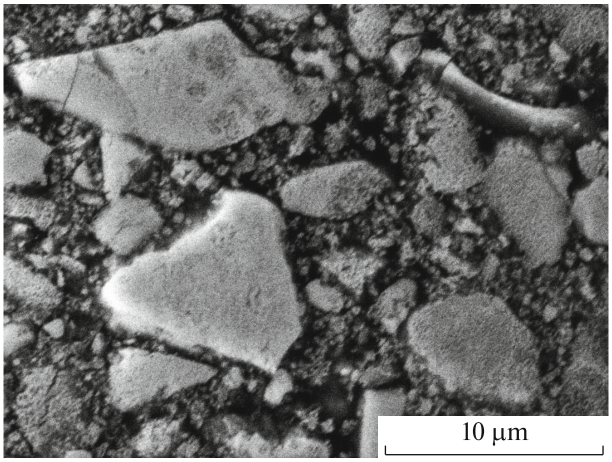

**Fig. 2.** Micrograph of the $Mg_{0.5}Zr_2(AsO_4)_{1.5}(PO_4)_{1.5}$ sample.

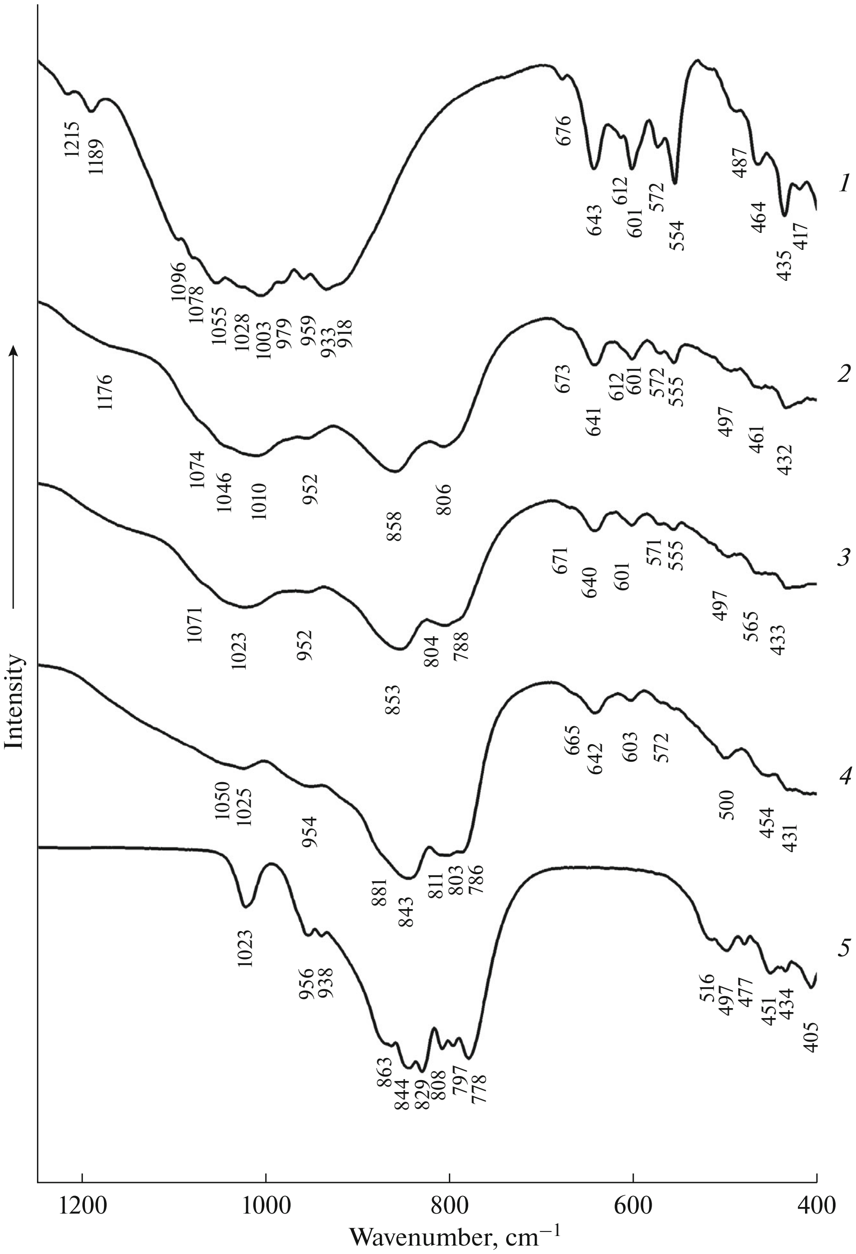

**Fig. 3.** IR spectra of $Mg_{0.5}Zr_2(AsO_4)_x(PO_4)_{3-x}$ with $x$ = (*1*) 0, (*2*) 1.0, (*3*) 1.5, (*4*) 2.0, and (*5*) 3.0.

positions. The stretching region of the phosphate ion ($x = 0$) contains seven peaks due to $\nu_3$ asymmetric vibrations (1003–1215 cm$^{-1}$) and four bands of $\nu_1$ symmetric vibrations (920–980 cm$^{-1}$). The bending region of the phosphate ion contains six bands of medium intensity due to $\nu_4$ asymmetric vibrations of the $PO_4^{3-}$ tetrahedra (550–680 cm$^{-1}$) and four bands of $\nu_2$ symmetric vibrations of the tetrahedra (415–480 cm$^{-1}$). The absorption bands of the arsenate ion ($x = 3$) are shifted to lower frequencies by 150–200 cm$^{-1}$ relative to the bands of the phosphate ion, in accordance with the increase in the mass of the central ion. Stretching modes of the $AsO_4^{3-}$ ion show up in the ranges 820–1025 ($\nu_3$) and 775–810 cm$^{-1}$ ($\nu_1$), and its bending modes are observed between 400 and 520 cm$^{-1}$ ($\nu_4$).

The IR spectra of the solid solutions show absorption bands of both the $PO_4^{3-}$ or $AsO_4^{3-}$ ions present in their structure. Throughout the spectral range studied, the spectra of all intermediate compositions have broader bands in comparison with those of the end-members of the solid solution series, suggesting that the tetrahedral site is occupied by phosphorus and arsenic atoms at random. The spectra well illustrate the decrease in the percentage of phosphate ions

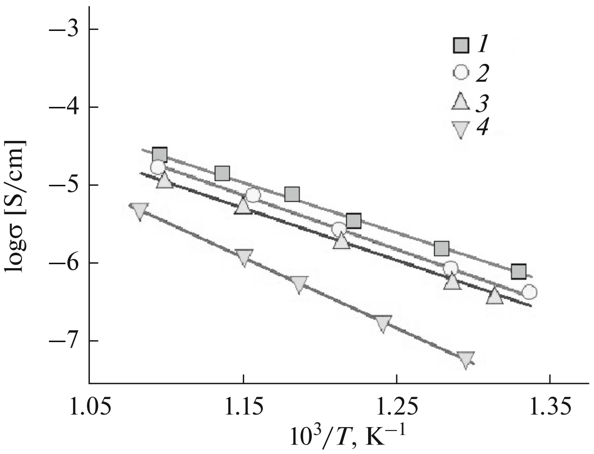

**Fig. 4.** Arrhenius plots of electrical conductivity for the $Mg_{0.5}Zr_2(AsO_4)_x(PO_4)_{3-x}$ solid solutions with $x$ = (*1*) 0, (*2*) 1.0, (*3*) 2.0, and (*4*) 3.0.

(stretching vibrations between 915 and 1215 cm$^{-1}$) and the increase in the percentage of the arsenate component (stretching vibrations between 775 and 1020 cm$^{-1}$) across the solid solution series. The gradual shift of the absorption bands of the $AsO_4$ tetrahedra to lower frequencies (858 cm$^{-1}$ at $x = 1$ and 843 cm$^{-1}$ at $x = 2$) with increasing arsenic content on the tetrahedral site attests to the formation of a continuous series of $Mg_{0.5}Zr_2(AsO_4)_x(PO_4)_{3-x}$ substitutional solid solutions, in agreement with the above X-ray diffraction results.

The ionic conductivity of the $Mg_{0.5}Zr_2(AsO_4)_x(PO_4)_{3-x}$ solid solutions was measured in the temperature range 740–950 K (Fig. 4). Extrapolation of the impedance plots obtained at lower temperatures resulted in high uncertainty. The samples with $0 \le x \le 2$ had nearly the highest conductivity: (1–3) × $10^{-5}$ S/cm at 900 K and (1–1.7) × $10^{-6}$ S/cm at 773 K. These values are comparable to the ionic conductivity of $Mg_{0.5}Zr_2(PO_4)_3$ [11] but lower than that of Zn-, Al-, and Fe-doped magnesium zirconium phosphates [12, 13]. Note that there is a pronounced tendency for the ionic conductivity to decrease as the degree of arsenic substitution for phosphorus increases. The observed behavior is most likely due to an increase in the size of the conduction channels in the structure of the material. It is known that there is an optimal relationship between the sizes of the conduction channels and migrating ions [9]. It seems likely that the slightly smaller size and larger charge of magnesium ions in comparison with lithium ions result in a relationship opposite to that observed previously for $LiZr_2(AsO_4)_x(PO_4)_{3-x}$ materials [15]. The present results are consistent with the finding reported by Halim et al. [14] that the electrical conductivity of the material in question increases with decreasing conduction channel size.

## CONCLUSIONS

$Mg_{0.5}Zr_2(AsO_4)_x(PO_4)_{3-x}$ samples have been synthesized and characterized by X-ray diffraction and IR spectroscopy. The results indicate the formation of a continuous series of solid solutions with the SW structure. Their unit-cell parameters increase linearly as $P^{5+}$ is replaced by $As^{5+}$, a larger sized ion. $P^{5+}$ substitution for $As^{5+}$, a larger sized ion, leads to a decrease in the ionic conductivity of $Mg_{0.5}Zr_2(AsO_4)_x(PO_4)_{3-x}$. The reduction in ionic conductivity seems to be caused by the increase in the size of the conduction channels, which are too large for $Mg^{2+}$ migration.

## ACKNOWLEDGMENTS

This work was supported by the Russian Foundation for Basic Research, project nos. 15-03-00716 and 16-33-00888.

## REFERENCES

1. Pet'kov, V.I., Complex phosphates formed by metal cations in oxidation states I and IV, *Russ. Chem. Rev.,* 2012, vol. 81, no. 7, pp. 606–637.
2. Yaroslavtsev, A.B. and Stenina, I.A., Complex phosphates with the NASICON structure ($M_xA_2(PO_4)_3$), *Russ. J. Inorg. Chem.,* 2006, vol. 51, suppl. 1, pp. S97–S116.
3. Ivanov-Shitz, A.K. and Murin, I.V., *Ionika tverdogo tela* (Solid-State Ionics), St. Petersburg: S.-Peterburg. Gos. Univ., 2001, vol. 1.
4. Aono, H., Sugimoto, E., Sadaoka, Y., Imanaka, N., and Adachi, G., Ionic-conductivity of solid electrolytes based on lithium titanium phosphate, *J. Electrochem. Soc.,* 1990, vol. 137, no. 4, pp. 1023–1027.
5. Best, A.S., Forsyth, M., and MacFarlane, D.R., Stoichiometric changes in lithium conducting materials based on $Li_{1+x}Al_xTi_{2-x}(PO_4)_3$: impedance, X-ray and NMR studies, *Solid State Ionics,* 2000, vols. 136–137, pp. 339–344.
6. Adachi, G., Imanaka, N., and Aono, H., Fast $Li^+$ conducting ceramic electrolytes, *Adv. Mater.,* 1996, vol. 8, no. 2, pp. 127–135.
7. Stenina, I.A., Kislitsyn, M.N., Pinus, I.Yu., Arkhangel'skii, I.V., Zhuravlev, N.A., and Yaroslavtsev, A.B., Phase transformations and cation mobility in NASICON lithium zirconium double phosphates $Li_{1\pm x}Zr_{2-x}M_x(PO_4)_3$ (M = Sc, Y, In, Nb, Ta), *Russ. J. Inorg. Chem.,* 2005, vol. 50, no. 6, pp. 906–911.
8. Muldoon, J., Bucur, C.B., Oliver, A.G., Sugimoto, T., Matsui, M., Kim, H.S., Allred, G.D., Zajicek, J., and Kotani, Y., Electrolyte roadblocks to a magnesium rechargeable battery, *Energy Environ. Sci.,* 2012, vol. 5, pp. 5941–5950.
9. Yaroslavtsev, A.B., Solid electrolytes: main prospects or research and development, *Russ. Chem. Rev.,* 2016, vol. 85, no. 11, pp. 1255–1276.
10. Tamura, S., Yamane, M., Hoshino, Y., and Imanaka, N., Highly conducting divalent $Mg^{2+}$ cation solid electrolytes with well-ordered three-dimensional network

structure, *J. Solid State Chem.,* 2016, vol. 235, no. 1, pp. 7–11.

11. Anuar, N.K., Adnan, S.B.R.S., and Mohamed, N.S., Characterization of $Mg_{0.5}Zr_2(PO_4)_3$ for potential use as electrolyte in solid state magnesium batteries, *Ceram. Int.,* 2014, vol. 40, no. 8, pp. 13 719–13 727.
12. Anuar, N.K. and Mohamed, N.S., Structural and electrical properties of novel $Mg_{0.9+0.5y}Zn_{0.4}Al_yZr_{1.6-y}(PO_4)_3$ ceramic electrolytes synthesized via nitrate sol–gel method, *J. Sol–Gel Sci. Technol.,* 2016, vol. 80, pp. 249–258.
13. Anuar, N.K., Adnan, S.B.R.S., Jaafar, M.H., and Mohamed, N.S., Studies on structural and electrical properties of $Mg_{0.5+y}(Zr_{2-y}Fe_y)_2(PO_4)_3$ ceramic electrolytes, *Ionics,* 2016, no. 22, pp. 1125–1133.
14. Halim, Z.A., Adnan, S.B.R.S., and Mohamed, N.S., Effect of sintering temperature on the structural, electrical and electrochemical properties of novel $Mg_{0.5}Si_2(PO_4)_3$ ceramic electrolytes, *Ceram. Int.,* 2016, vol. 42, no. 3, pp. 4452–4461.
15. Pet'kov, V.I., Sukhanov, M.V., Shipilov, A.S., Kurazhkovskaya, V.S., Borovikova, E.Yu., Pinus, I.Yu., and Yaroslavtsev, A.B., Synthesis and properties of $LiZr_2(AsO_4)_3$ and $LiZr_2(AsO_4)_x(PO_4)_{3-x}$, *Inorg. Mater.,* 2014, vol. 50, no. 3, pp. 263–272.
16. Jouanneaux, A., Verbaere, A., Piffard, Y., Fitch, A.N., and Kinoshita, M., How to distinguish between monoclinic distortions of Nasicon and $Sc_2(WO_4)_3$ structure types from X-ray-powder patterns—crystal-structure of $Ni_{0.5}Zr_2(PO_4)_3$, *Eur. J. Solid State Inorg. Chem.,* 1991, vol. 28, pp. 683–699.
17. Pet'kov, V.I., Shipilov, A.S., Borovikova, E.Yu., Boldyrev, K.N., and Koval'skii, A.M., Synthesis and X-ray crystallographic and IR-spectroscopic study of complex alkaline earth zirconium arsenates, *Russ. J. Inorg. Chem.,* 2017, vol. 62, no. 2, pp. 218–223.
18. Pet'kov, V.I., Kurazhkovskaya, V.S., Orlova, A.I., and Spiridonova, M.L., Synthesis and crystal chemical characteristics of the structure of $M_{0.5}Zr_2(PO_4)_3$ phosphates, *Crystallogr. Rep.,* 2002, vol. 47, no. 5, pp. 736–743.

*Translated by O. Tsarev*